



A quantitative assessment of the mechanical strength of the polar pteropod *Limacina helicina antarctica* shell

Clara M. H. Teniswood¹, Donna Roberts², William R. Howard³, and Jodie E. Bradby^{1*}

¹Research School of Physics and Engineering, The Australian National University, Canberra, ACT 0200, Australia

²Antarctic Climate and Ecosystems Cooperative Research Centre, University of Tasmania, Private Bag 80, Sandy Bay, TAS 7001, Australia

³Research School of Earth Sciences, The Australian National University, Canberra, ACT 0200, Australia

*Corresponding Author: tel: +61 2 61254916; fax: +61 2 61250511; e-mail: jodie.bradby@anu.edu.au

Teniswood, C. M. H., Roberts, D., Howard, W. R., and Bradby, J. E. 2013. A quantitative assessment of the mechanical strength of the polar pteropod *Limacina helicina antarctica* shell. – ICES Journal of Marine Science, 70: 1499–1505.

Received 1 February 2013; accepted 30 April 2013; advance access publication 20 August 2013.

This work directly measures the mechanical properties of pteropod shells collected from the Southern Ocean on the 2007 midsummer Subantarctic Zone Sensitivity to Environmental Change (SAZ-Sense) voyage. Shells from the common Southern Ocean pteropod *Limacina helicina antarctica* were subjected to mechanical analyses in combination with detailed morphological studies. Average hardness and modulus of 2.30 ± 0.07 GPa and 45.27 ± 0.91 GPa, respectively were calculated from several hundred nanoindentation measurements taken from multiple positions across twelve shells of the same species collected under identical conditions. Quantitative data such as these are critical to establish a reference point for future comparative studies and to both understand and evaluate the implications of further ocean acidification on the structural integrity of these common polar calcifiers, particularly in light of their role in the Southern Ocean carbon cycle and food web.

Keywords: calcifying, mechanical properties, nanoindentation, ocean acidification, pteropods, Southern Ocean.

Introduction

The oceans have absorbed nearly 40% of the anthropogenic carbon dioxide (CO₂) released into the atmosphere since the Industrial Revolution (Sabine *et al.*, 2004). The addition of CO₂ affects ocean chemistry by decreasing both the carbonate ion availability and the pH of the surface ocean (Caldeira and Wickett, 2003; Feely *et al.*, 2004). This phenomenon, known as ocean acidification, is predicted to affect polar waters first. Models suggest these polar waters will become undersaturated with respect to the aragonite polymorph of calcium carbonate by 2050, associated with a drop in ocean pH to 7.9 (Orr *et al.*, 2005; McNeil and Matear, 2008). Despite being a key question in ocean acidification research, we still have a limited understanding of how calcifying organisms will respond to a high-CO₂ ocean (Doney *et al.*, 2009; Ries *et al.*, 2009; Kroeker *et al.*, 2010). Many studies have suggested calcium carbonate shell formation will be reduced throughout a range of calcifying organisms including planktonic foraminifera (Spero *et al.*, 1997; Bijma *et al.*, 1999, 2002; Moy *et al.*, 2009), corals (Gattuso *et al.*, 1998; Kleypas *et al.*, 1999; Gattuso and Buddemeier, 2000), some coccolithophorids (Riebesell *et al.*, 2000; Zondervan *et al.*, 2001) and pteropods (Comeau *et al.*, 2009; Lischka, 2012; Manno *et al.*,

2012). Calcification has a vital role in the marine carbon and alkalinity cycles, where aragonite precipitation and dissolution is a prominent component of the upper-ocean alkalinity cycle (Betzer *et al.*, 1984; Gangstø *et al.*, 2008). In the case of pteropods, a number of studies have applied qualitative and semi-quantitative metrics to shell calcification and preservation state (e.g. Gerhardt and Henrich, 2001; Manno *et al.*, 2007; Roberts *et al.*, 2011; Bednaršek *et al.*, 2012).

The thecosomatous (shelled) pteropods play an important role in marine ecosystems (Lalli and Gilmer, 1989). When abundant, pteropods are significant grazers on phytoplankton and smaller mesozooplankton. Pteropods produce shells from aragonite, which is a brittle mineral phase of calcium carbonate and metastable under oceanic conditions. Aragonite is more vulnerable to dissolution than calcite, and thus more susceptible to ocean acidification than calcite in terms of shell formation, as aragonite undersaturation will be crossed at a higher carbonate ion concentration than for calcite (Mucci, 1983). Indeed, laboratory, modelling and field studies on polar pteropods have indicated that shell dissolution will occur rapidly as polar oceans becomes undersaturated with aragonite (Orr *et al.*, 2005; Manno *et al.*, 2007; Comeau *et al.*, 2009;

Bednaršek *et al.*, 2012). Thus, quantifying the current distribution, abundance, seasonal flux and mechanical properties of Southern Ocean pteropods is crucial, as they are likely to be among the most vulnerable organisms to the effects of ocean acidification. Work quantifying the distribution, abundance and seasonal flux of pteropods in the Subantarctic Zone (SAZ) has been completed to provide a benchmark against which to monitor future changes in SAZ pteropod communities (Howard *et al.*, 2011). However, to date there have been no studies examining the mechanical properties of the shells of this set of organisms. Moreover, measuring the structural and mechanical properties, such as hardness and modulus, of the shells of calcifiers is one important method of determining changes in the structural integrity, and thus survival, of these at-risk organisms. This study thus aims to establish a reference point for the mechanical properties of pteropod shells collected from the SAZ.

Although there have been no studies on the mechanical characteristics of Southern Ocean pteropods, there are reports of the mechanical properties of other marine calcified shells. Taylor and Layman (1972) first measured the mechanical properties of bivalve shell structures with an array of microhardness, compression, bend and impact tests. They showed that in some structures, such as aragonite prisms, there was significant variation in the microhardness observed from species to species. They also noted that there was no significant variation in the microhardness of prismatic or crossed-lamellar structures with different orientations. Nanoindentation is now a well-established technique whereby the localized mechanical properties of a sample can be measured by pushing a sharp tip down into a material with a defined force whilst continuously measuring the resultant penetration depth (Doerner and Nix, 1986). Young's Modulus and hardness are routinely calculated from nanoindentation measurements. The Young's modulus is a measure of a material's ability to deform elastically and is defined as the ratio of the tensile stress over strain in the elastic regime. Nanoindentation systems typically calculate the Young's modulus by measuring the elastic recovery of the material on the withdrawal of the indenter tip (i.e. on unloading). Hardness is defined as "resistance to permanent deformation" and is calculated from the force and the projected contact area. Though developed primarily for nonbiological material analyses, nanoindentation is becoming a powerful tool for measuring the mechanical properties of many biomaterials, as it can measure the hardness and Young's modulus at scales appropriate to many biomaterials and at site-specific locations. The indented regions can then be further characterized with techniques such as electron microscopy, thus providing important information about the structure–property relations of such systems. This approach has been extensively applied to many hard biomaterials including teeth and bone (Lewis and Nyman, 2008), insect exoskeletons (Enders *et al.*, 2004; Barbakadze *et al.*, 2006) and a number of soft biomaterials of both technical and fundamental interest, such as silk fibres (Ebenstein and Wahl, 2006). Nanoindentation has also been employed to study nacre, the inner iridescent layer of many marine mollusc shells. Nacre is of particular interest due to its extraordinary combination of strength and fracture toughness despite being composed of mainly (>95%) brittle aragonite (Espinosa *et al.*, 2011). The mechanical properties of this hierarchically-structured biomaterial have been well studied using a range of techniques including Atomic Force Microscopy and nanoindentation with the aim of understanding the structure–property relations of nacre for potential technological applications (Bruet *et al.*, 2005; Katti *et al.*, 2006; Espinosa *et al.*, 2011). Nanoindentation has also been used to provide valuable insights into the mechanical properties of the tropical pteropod *Cavolinia uncinata*, which has an

interlocked helical nanofibre aragonite structure (Zhang *et al.*, 2011). The modulus and hardness measured from that shell structure revealed that the properties on the transverse cross-section are much higher than the section parallel to the shell surface, which appears to allow the shells to be somewhat flexible as well as providing excellent fracture toughness (Zhang *et al.*, 2011). The shells of polar pteropods are similarly composed of aragonite. The outer shell morphology of two species of polar pteropods, the Arctic *Limacina helicina* and the Antarctic *Limacina helicina antarctica* forma *antarctica*, have been studied by Sato-Okoshi *et al.* (2010). Adult Antarctic pteropod shells were shown to consist of three layers: a crossed-lamellar layer between an inner and a thin outer prismatic layer. Axial ribbed growth lines were observed on the surface of the shells and a thin periostracal layer covered the calcareous shell. Mollusc shells are thought to contain ~5% biological protein materials (Hare and Abelson, 1964), but there has been no work on the nature or composition of these proteins in this organism.

Although the mechanical properties of calcifying organisms, such as pteropods in polar waters, are of key interest in terms of ocean acidification, there are currently no reports in the literature on such properties. In this work, we use nanoindentation to measure the hardness and modulus of the Southern Ocean pteropod *Limacina helicina antarctica* (LHA), together with electron microscopy, to provide a series of reference measurements that aim to tackle the question of how mechanical properties of calcifiers will fare in a higher CO₂ ocean.

Material and methods

Sample collection

The set of *Limacina helicina antarctica* pteropods examined in this study were collected during the Subantarctic Zone Sensitivity to Environmental Change (SAZ-Sense) voyage, which covered an area from 44–54°S and 140–155°E between 17 January and 20 February 2007. The specimens were collected from Subantarctic Zone waters, bounded to the north by the Subtropical Front and to the south by the Polar Frontal Zone (Figure 1) [see Howard *et al.* (2011) for full SAZ-Sense collection site details]. A "Ringnet" and a "Rectangular Midwater Trawl (RMT) Net"

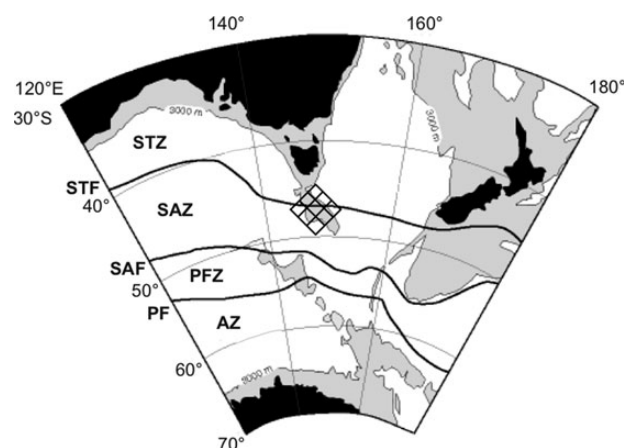


Figure 1. SAZ-Sense sample area (hatched diamond) in relation to the oceanographic fronts and zones of the Southern Ocean (after Rintoul and Bullister, 1999). STZ, Subtropical Zone; STF, Subtropical Front; SAZ, Subantarctic Zone; SAF, Subantarctic Front; PFZ, Polar Frontal Zone; PF, Polar Front; AZ, Antarctic Zone.

(Roe *et al.*, 1980; Pommeranz *et al.*, 1982) were used to collect samples to maximize sample collection.

The ringnet was deployed vertically at varying times of day between 0 and 100 m depth at a speed of 0.5 ms^{-1} . The net had a mouth area of 0.8 m^2 and was fitted with a $150\text{-}\mu\text{m}$ mesh and a 20-l, 0.3-m wide non-filtering cod-end bucket.

Each RMT deployment consisted of two 15-min trawls. On some occasions only one part of the trawl was successful as a result of damage to the net and/or cod-end and on two occasions a second trawl was not undertaken. The RMT1 net (1 m^2 mouth area fitted with $150\text{-}\mu\text{m}$ mesh) and the RMT8 net (8-m^2 net opening with 2-mm mesh) were deployed for horizontal tows between 0- and 150-m water depths at speeds of 0.5–1.9 knots.

Sample preservation and processing

A 2-l subsample from the ringnet cod-end and all of the RMT 1 and 8 cod-end samples were sieved through a $150\text{-}\mu\text{m}$ mesh sieve. Pteropods were optically identified and preserved in 100% ethanol for 24–48 h, after which they were washed and refreshed with new 100% ethanol and preserved at 4°C . It is important to note that the samples used in this study were not treated further (e.g. subjected to a peroxide (bleach) clean) and thus original shells with organic matter intact were retained.

To prepare each shell for mechanical measurement, whole specimens were dried at room temperature in a desiccator for $\sim 24 \text{ h}$ before being embedded in epoxy resin and hardener (EpoxySet, Allied). To reveal a cross-section of the shell wall, the samples were polished using a series of silicon carbide papers followed by a final polish with a silk cloth embedded with $3\text{-}\mu\text{m}$ and $1\text{-}\mu\text{m}$ diamond pastes.

Sample analysis

The mechanical properties of the pteropod shells were determined using nanoindentation. A Hysitron TriboIndenter with a pointed (Berkovich) diamond tip (with typical diameter of $100\text{--}200 \text{ nm}$) was used. The tip area file and instrument compliance was calculated using a standard of fused silica. A maximum load of 5 mN was applied to the shell cross-section over a 30-s interval and unloaded over 10 s . A set of 12 individual pteropods were indented, in various regions of the shell cross-sections, totalling approximately 600 individual indentations. The hardness and modulus was calculated using the software built into the Hysitron instrument based on the Oliver and Pharr method (Oliver and Pharr, 1992). This method fits the unloading segment of the curve to a power law relation to calculate the contact depth, from which the contact area can be obtained. The hardness (H) is then given by:

$$H = P_{\max}/A,$$

where P_{\max} is the maximum load and A is the projected area of the residual indent impression (contact area) calculated by the measured depth and known tip area function. The elastic modulus (E) is calculated using the unloading stiffness ($S = dP/dh$) and contact area. It should be noted that the modulus presented in this work is the “reduced” modulus, as there is a small contribution in the measurement from the properties of the diamond tip. The absolute Young’s modulus of a sample (E) can be obtained given the Poisson’s ratio of the material:

$$1/E_{\text{reduced}} = (1 - \nu^2)/E + (1 - \nu_i^2)/E_i,$$

where E , ν , E_i and ν_i are the Young’s moduli and Poisson’s ratios of the material and indenter respectively. However as there is no way to accurately measure the Poisson’s ratio of the pteropod shells, the modulus presented in this work is the reduced modulus. This is standard practice in most nanoindentation studies, as the effect of the tip deformation is very small and estimating Poisson’s ratio would introduce an unknown degree of error into the measurements.

Each nanoindentation data set was imaged to determine the local surface morphology and shell orientation using a FEI Quanta 600 MLA environmental scanning electron microscope (ESEM) in low vacuum mode at 10 kV . No coating was used. Whole shells that were not embedded in epoxy were also imaged.

Results

The *Limacina helicina antarctica* shells analysed in this work were found to have a diameter of $1\text{--}2 \text{ mm}$ (Figure 2). Axial ribs were observed on the shell surface (Figure 2), which is in agreement with previous reports by Sato-Okoshi *et al.* (2010). The thickness of the shell wall cross-sections were measured via ESEM and ranged from $5\text{--}30 \text{ }\mu\text{m}$ depending on shell region (Figure 3).

A typical nanoindentation curve taken from a shell wall shows the plot of applied load and measured depth (Figure 4). The mechanical behaviours of individual regions were found to vary within this relatively large dataset of approximately 600 indentations across the 12 shells. In some areas the indenter penetrated the shell to a depth of $\sim 700 \text{ nm}$ indicating that specific region was very soft, while in other areas the indenter only penetrated $\sim 200 \text{ nm}$ into the surface indicating this region was relatively harder. This variability occurred across each shell in the sample set. The average hardness and modulus values and the associated standard error for the entire sample set (~ 600 indents across 12 shells) were calculated from the indentation data. The average hardness for individual shells ranges from $0.87 \pm 0.09 \text{ GPa}$ to $4.44 \pm 0.20 \text{ GPa}$ (Figure 5a), and the average modulus ranges from $29.24 \pm 2.1 \text{ GPa}$ to $64.69 \pm 1.9 \text{ GPa}$ (Figure 5b). The average of all ~ 600 measurements was calculated and is shown as the blue line on both plots. The overall average hardness is $2.30 \pm 0.07 \text{ GPa}$, and the overall average modulus is $45.27 \pm 0.91 \text{ GPa}$. It is interesting to consider if such hardness variations may be caused by local differences in ocean chemistry experienced by the pteropods over their lifetime due to seasonal variations or daily migrations through the water columns.

The residual indent impressions in the polished shell cross-section were imaged in the ESEM (Figure 3) in an attempt to map the local morphology of the regions being probed with the measured mechanical properties. Indeed, the morphology of the polished shell cross-sections was found to vary considerably both within each shell and across the whole sample set. Some areas appeared “rough” with long rod-like crystals visible (Figure 3a), while others were very smooth (Figure 3b). In addition many regions probed with an array of indentations displayed a mixture of these two morphologies (Figure 3c). Information about the local morphology of each array of indents was correlated with the respective nanoindentation data. However, the variation in morphology was found not to be correlated with the mechanical data calculated. The position of the indents within each shell (e.g. in the middle or on the outer layer) and region (e.g. on the embryonic shell or outer whorl) was also carefully studied to see if this had any relation to the mechanical properties but again, no correlation was seen. Thus the observed variation in the localized mechanical properties is not related to

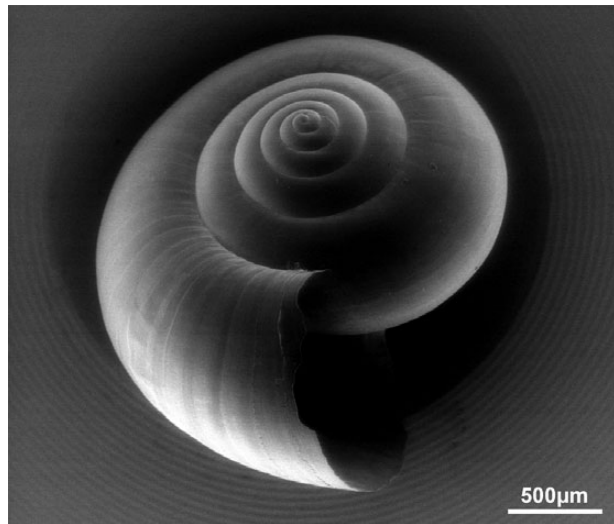


Figure 2. Environmental scanning electron microscope (ESEM) image of a whole pteropod shell that had been stored in ethanol since collection in 2007.

the surface morphology but to naturally occurring subsurface microstructural variations.

Discussion

Pteropod research to date has relied on the use of measurements (such as short-term laboratory experiments or shell flux of *in situ* populations) to detect changes in calcification rates and to make inferences about likely population changes under continuing ocean acidification (Orr *et al.*, 2005; Comeau *et al.*, 2009; Roberts *et al.*, 2011; Bednaršek *et al.*, 2012). Although these studies have provided much important information about the likely impact of changing ocean chemistry on calcareous marine organisms, such approaches have not addressed the fundamental questions about the structural composition of these calcifying marine creatures and how changes to pH will affect their integrity and hence their ability to both form and maintain shells. Laboratory experiments are limited by the inability to keep pteropods alive out of their natural environment for more than a month (Comeau *et al.*, 2009; Lischka *et al.*, 2011). In addition, experimental treatments are sudden and do not allow for possible generational adaptation (Bednaršek *et al.*, 2012). Hence, measurements of the mechanical properties of pteropods collected from natural populations provide a good indication of the resistance to deformation, which in this case may be vital for the organisms' survival. In this research, the key question of the structural integrity is addressed using nanoindentation as a means of measuring their mechanical properties. The suitability of this technique is discussed in terms of what the properties of hardness and modulus probe and how the organic component of the shell affects such properties.

In terms of mechanical properties, “hardness” is regularly quoted in order to characterize materials. The search for so-called “superhard” materials is naturally defined by this concept, despite the fact that hardness is not a fundamental material property as it cannot be calculated from a unit cell or a detailed understanding of the local bonding of the atoms. Hardness is best defined as a measure of the resistance of a material to permanent deformation. As the function of the pteropod shell is to provide protection,

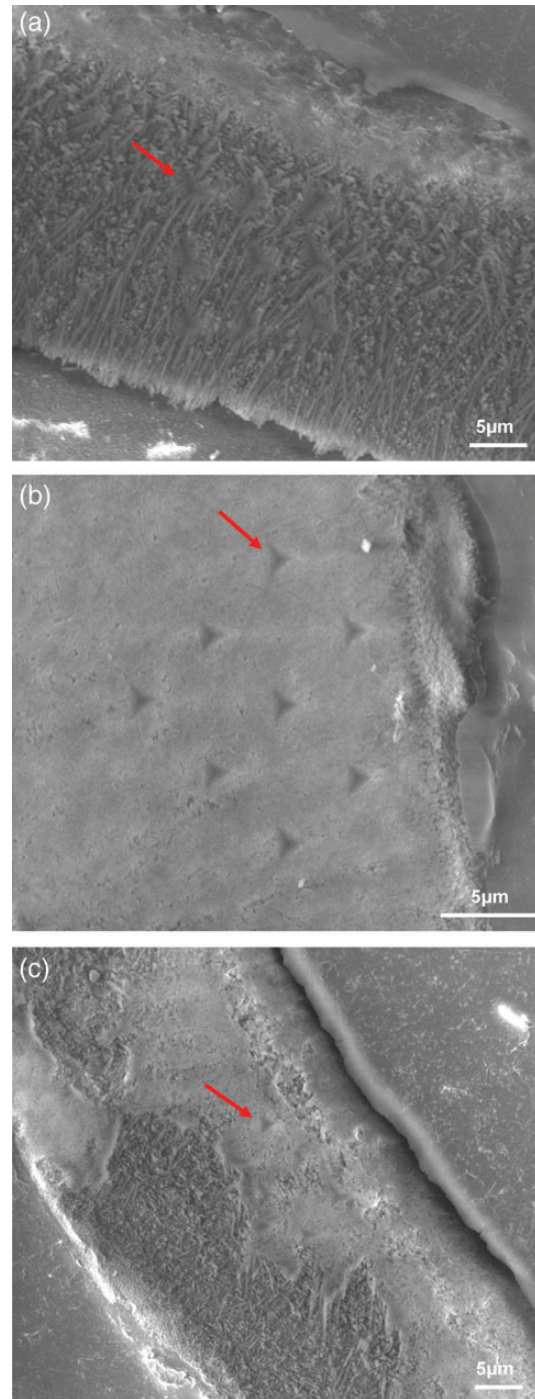


Figure 3. ESEM images of indent arrays in differing surface morphologies: (a) “rough”, long rod-like crystals, (b) “smooth”, (c) combination of “smooth” and “rough”. [(b) and (c) are from the same individual shell.]

measuring the hardness of such shells seems an appropriate measure of the shell's ability to perform its function. However given that hardness is not a fundamental material property, the value obtained from indentation tests depend heavily on the details of the testing regime. For example, different indentation tip shapes (i.e. spherical or 3- or 4-sided pyramid) and maximum

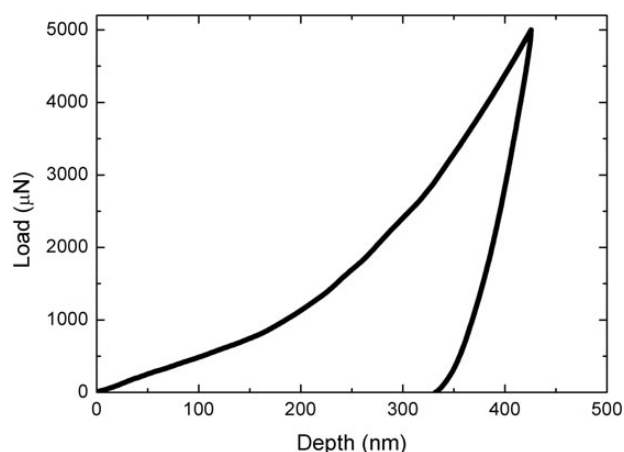


Figure 4. Typical nanoindentation load–depth plot from an LHA pteropod shell collected in 2007.

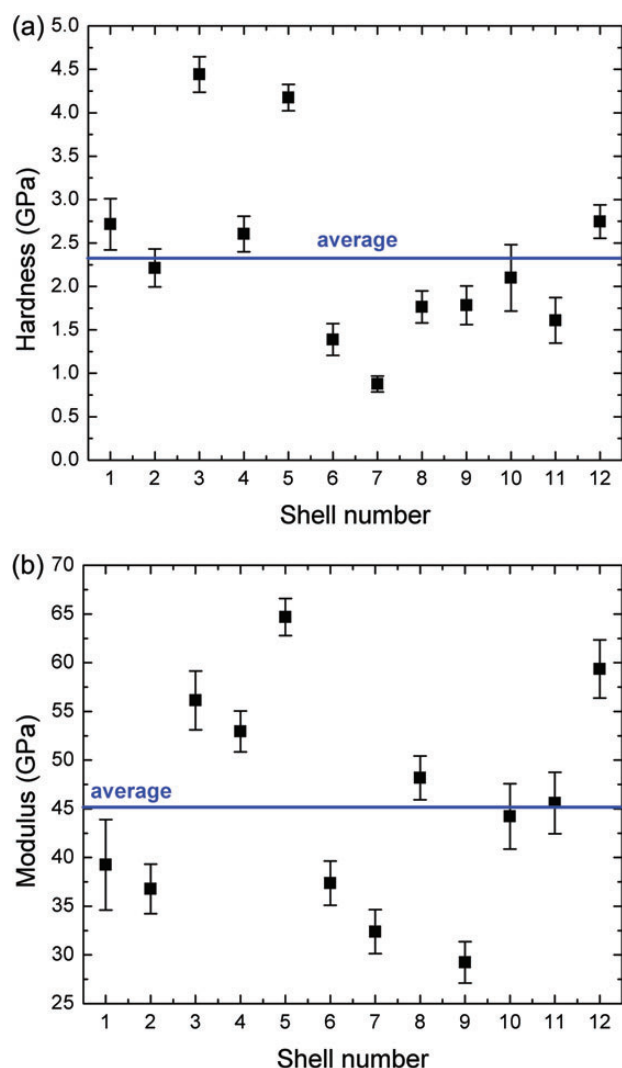


Figure 5. The average hardness and modulus for each shell in the sample set. The average of all data obtained is shown. A colour version of this figure can be accessed online.

loads can result in different measured values of the hardness (Fischer-Cripps, 2004).

In contrast to hardness, the Young's modulus is a fundamental property. It is commonly measured as the ratio between the stress and strain of a material. Primarily the modulus is a measure of the elasticity of a material and, unlike hardness, it can be measured in the elastic regime before permanent deformation has occurred. However, the measured Young's modulus can also vary according to the testing method. In this case the most significant factors are the loading and unloading rates, which are of particular importance for polymers. As the shell samples studied here contain ~5% organic matter, this factor needs to be considered when making comparisons with other work.

Therefore, in order to make mechanical measurements that are useful for comparative studies, there are a number of parameters that need to be considered for indentation testing. The selection of both the indenter tip shape and maximum load are very important. Ideally the selected tip/load combination should induce plastic (i.e. permanent) deformation without inducing failure (cracking) in the sample. In addition, the area being probed and the maximum depth of the tip should be scaled to both the size of the sample and the degree of surface roughness. A well-known rule of thumb in the field states that the depth should not exceed more than 10% of the sample thickness (Tsui *et al.*, 1999), and the maximum depth of the test also needs to very comfortably exceed the level of surface roughness (Fischer-Cripps, 2004).

All of the above factors were taken into consideration when the indentation testing conditions presented here were established. At a maximum load of 5 mN with a Berkovich indenter, the maximum depth was measured between ~200 to ~700 nm. The ESEM analysis of the residual indent impressions revealed that this load did not induce any cracking. Thus we suggest that these conditions are appropriate for measuring the mechanical properties of these samples and can be easily repeated with shells from later years to monitor any possible changes in this set of mechanical properties.

The influence of the organic component on the mechanical properties of the shells is also worth considering. A suggested explanation for the measured variations in the mechanical properties of the shells is the presence of the organic matrix. However as the organic matrix is essentially homogenous throughout the shell and only ~5% of the structure overall, it is likely that a similar volume of organic matter is probed during each indentation and thus this is unlikely to cause large variations in the mechanical responses. Yet the organic matter, even in the dehydrated form tested in this work, clearly plays a vital role in strengthening the shell. Indentation of a classic brittle ceramic such as aragonite (Jackson *et al.*, 1988) under the same conditions would evidently cause cracking. However, no cracks were visible around the residual indents and no signs of cracking, such as discontinuities in the load–unload data, were observed in this work.

In addition, the orientation of the shell does not appear to result in different hardness or modulus measurements. This is not surprising as the majority of the sample has a crossed-lamellar structure, and little variation in the hardness measured between different orientations was noted by Taylor and Layman (1972) in these structures. Thus the variation in the localized mechanical properties is attributed to the natural variation in the biomaterial being tested.

It is further interesting to compare the mechanical data obtained in this study with that of other shell structures published in the literature (Table 1). The most widely studied shell structure is nacre, which, like the *Limacina helicina antarctica* pteropod shell studied

Table 1. Mechanical properties of shells measured by nanoindentation using a Berkovich tip.

Species	Structure	Hardness (GPa)	Modulus (GPa)	Load (μN)	Notes
<i>Limacina helicina antarctica</i> (this work)	Aragonite: crossed-lamellar & prismatic	2.30 ± 0.07	45.27 ± 0.91	5000	
Pteropod <i>Cavolinia uncinata</i> (Zhang et al., 2011)	Aragonite: helical nanofibres	5.2 ± 0.4 5.6 ± 0.3	85.9 ± 2.7 51.5 ± 1.6	1200–1300	Transverse to shell cross-section Parallel to shell surface
<i>Trochus niloticus</i> (Bruet et al., 2005)	Aragonite: nacre	10.8 ± 1.5 8.7 ± 1.4	114.0 ± 8.8 103.0 ± 10.1	1000	Freshly cleaved Samples incubated in artificial seawater
<i>Haliotis rufescens</i> (Katti et al., 2006)	Aragonite: nacre	0.69–19.32 1.32–3.1	14.85–113.74 40.95–56.71	10 10 000	

here, is also composed of aragonite with an organic matrix of ~5 wt%. However, the structure of nacre is very different from the LHA structure, as it comprises polygonal platelets separated by an organic matrix (Bruet et al., 2005). The hardness of nacre has been measured to be 8.7–10.8 GPa, and the modulus measured to be 103–114 GPa, with a maximum indentation load of 1000 μN (Bruet et al., 2005). Another study by Katti et al. (2006) found the hardness and modulus to be 1.32–3.1 GPa and 40.95–56.71 GPa respectively, with a 10 000 μN maximum indentation load. Although the results and variations from this work do come close to the reported properties of nacre, the apparent inconsistencies in the reported values illustrate the importance of adopting a standardized indentation measurement procedure.

A comparison of mechanical properties of the LHA-pteropod presented in this work with those of a tropical species of pteropod is also possible (Table 1). It appears that the Southern Ocean LHA shells are significantly “softer” than the shells of the tropical pteropod *Cavolinia uncinata* (CU) (Zhang et al., 2011). The tropical pteropods had a hardness and modulus of 5.2–5.6 GPa and 51.5–85.9 GPa, respectively, depending on whether the shell was indented on the transverse cross-section or parallel to the shell surface (Table 1; Zhang et al., 2011). Again, a likely explanation for this difference in mechanical behaviour can be attributed to an unusual interlocked helical nanofibre aragonite structure found in the CU pteropod compared with the layer cross-laminar structure in the LHA species. This indicates that the structural arrangement of aragonite likely dominates the mechanical properties of the shell. Thus, little useful information about the mechanical properties of one species can be extrapolated from those of another species, even if the compositions are roughly the same (aragonite plus ~5% organic matter).

Over coming decades, aragonite undersaturation is predicted to detrimentally affect planktonic marine communities of high-latitude waters, and indeed some impacts have already been inferred (e.g. Moy et al., 2009). The rate and magnitude of these observed and anticipated changes (Southern Ocean surface waters undersaturated by 2050: McNeil and Matear, 2008) highlight the urgent need for monitoring at-risk calcifiers, such as Antarctic pteropods. It should be noted that these pteropods are rarely preserved in Southern Ocean sediments, and thus pre-industrial baselines on which to detect responses to ocean acidification are not available. However, nanoindentation may allow the effects of acidification to be measured while it occurs in our lifetime. The results presented here provide a valuable benchmark of the mechanical properties of these vulnerable pteropods and can act as a reference point for future comparative studies. In addition, a standard method of nanoindentation has been suggested for other such studies. Consistent experimental parameters are vital for researchers to make meaningful comparisons of data in order to evaluate the effects of ocean acidification on many important calcifying marine organisms.

Quantitative data such as these are critical for both understanding and evaluating the implications of further ocean acidification on the structural integrity, and thus the survival, of polar calcifiers.

Acknowledgements

The authors thank Master Scott Laughlin and the crew of the RSV “Aurora Australis”, and Australian Antarctic Division’s gear officers and fellow expeditioners for assistance with collection of samples from the Southern Ocean. Special thanks go to Karsten Goemann and Sandrin Feig of the Electron Scanning Facility at the Central Science Laboratory, University of Tasmania, for their friendly assistance with ESEM.

Funding

This work was supported by the Australian Government through the Department of Climate Change, the Australian Cooperative Research Centres Program and the Australian Antarctic Division (AAS Grant #2720).

References

Barbakadze, N., Enders, S., Gorb, S., and Arzt, E. 2006. Local mechanical properties of the head articulation cuticle in the beetle *Pachnoda marginata* (Coleoptera, Scarabaeidae). *Journal of Experimental Biology*, 209: 722–730.

Bednaršek, N., Tarling, G. A., Bakker, D. C., Fielding, S., Cohen, A., Kuzirian, A., McCorkle, D., et al. 2012. Description and quantification of pteropod shell dissolution: a sensitive bioindicator of ocean acidification. *Global Change Biology*, 18: 2378–2388.

Betzer, P. R., Byrne, R. H., Acker, J. G., Lewis, C. S., Jolley, R. R., and Feely, R. A. 1984. The oceanic carbonate system: a reassessment of biogenic controls. *Science*, 226: 1074–1077.

Bijma, J., Spero, H. J., and Lea, D. W. 1999. Reassessing foraminiferal stable isotope geochemistry: impact of the oceanic carbonate system (experimental results). In *Use of Proxies in Paleoclimatology*, pp. 489–512. Ed. by G. Fisher, and G. Wefer. Springer-Verlag, Berlin Heidelberg.

Bijma, J., Hönisch, B., and Zeebe, R. E. 2002. Impact of the ocean carbonate chemistry on living foraminiferal shell weight. *Geochemistry, Geophysics and Geosystems*, 3: 1064.

Bruet, B. J. F., Qi, H. J., Boyce, M. C., Panas, R., Tai, K., Frick, L., and Ortiz, C. 2005. Nanoscale morphology and indentation of individual nacre tablets from the gastropod mollusc *Trochus niloticus*. *Journal of Materials Research*, 20: 2400–2419.

Caldeira, K., and Wickett, M. E. 2003. Anthropogenic carbon and ocean pH. *Nature*, 425: 365.

Comeau, S., Gorsky, G., Jeffree, R., Teyssie, J. L., and Gattuso, J. P. 2009. Impact of ocean acidification on a key Arctic pelagic mollusc (*Limacina helicina*). *Biogeosciences*, 6: 1877–1882.

Doerner, M. F., and Nix, W. D. 1986. A method for interpreting the data from depth-sensing indentation instruments. *Journal of Materials Research*, 1: 601–609.

- Doney, S. C., Balch, W. M., Fabry, V. J., and Feely, R. A. 2009. Ocean acidification: a critical emerging problem for the ocean sciences. *Oceanography*, 22: 16–25.
- Ebenstein, D. M., and Wahl, K. J. 2006. Anisotropic nanomechanical properties of *Nephila clavipes* dragline silk. *Journal of Materials Research*, 21: 2035–2044.
- Enders, S., Barbakadse, N., Gorb, S. N., and Arzt, E. 2004. Exploring biological surfaces by nanoindentation. *Journal of Materials Research*, 18: 880–887.
- Espinosa, H. D., Juster, A. L., Latourte, F. J., Loh, O. Y., Gregoire, D., and Zavattieri, P. D. 2011. Tablet-level origin of toughening in abalone shells and translation to synthetic composite materials. *Nature Communications*, 2: 173.
- Feely, R. A., Sabine, C. L., Lee, K., Berelson, W., Kleypas, J., Fabry, V. J., and Millero, F. J. 2004. Impact of anthropogenic CO₂ on the CaCO₃ system in the oceans. *Science*, 305: 362–366.
- Fischer-Cripps, A. C. 2004. *Nanoindentation*. Springer Science+Business Media, New York, USA. 263 pp.
- Gangstø, R., Gehlen, M., Schneider, B., Bopp, L., Aumont, O., and Joos, F. 2008. Modeling the marine aragonite cycle: changes under rising carbon dioxide and its role in shallow water CaCO₃ dissolution. *Biogeosciences*, 5: 1057–1072.
- Gattuso, J.-P., Frankignoulle, M., Bourge, I., Romaine, S., and Buddemeier, R. 1998. Effect of calcium carbonate saturation of seawater on coral calcification. *Global and Planetary Change*, 18: 37–46.
- Gattuso, J.-P., and Buddemeier, R. 2000. Calcification and CO₂. *Nature*, 407: 311–312.
- Gerhardt, S., and Henrich, R. 2001. Shell preservation of *Limacina inflata* (Pteropoda) in surface sediments from the Central and South Atlantic Ocean: a new proxy to determine the aragonite saturation state of water masses. *Deep Sea Research I*, 48: 2051–2071.
- Hare, P. E., and Abelson, P. H. 1964. Proteins in mollusk shells. Report of the Director, Geophysics Laboratory, Carnegie Institution, Washington, 63, 267–270.
- Howard, W. R., Roberts, D., Moy, A. D., Lindsay, M. C. M., Hopcroft, R. R., Trull, T. W., and Bray, S. G. 2011. Distribution, abundance and seasonal flux of pteropods in the Sub-Antarctic Zone. *Deep Sea Research II*, 58: 2293–2300.
- Jackson, A. P., Vincent, J. F. V., and Tuner, R. M. 1988. The mechanical design of nacre. *Proceedings of the Royal Society of London. Series B*, 234: 415–440.
- Katti, K. S., Mohanty, B., and Katti, D. R. 2006. Nanomechanical properties of nacre. *Journal of Materials Research*, 21: 1237–1242.
- Kleypas, J., Buddemeier, R., Archer, D., Gattuso, J., Langdon, C., and Opdyke, B. 1999. Geochemical consequences of increased atmospheric carbon dioxide on coral reefs. *Science*, 284: 118–120.
- Kroeker, K. J., Kordas, R. L., Crim, R. N., and Singh, G. G. 2010. Meta-analysis reveals negative yet variable effects of ocean acidification on marine organisms. *Ecology Letters*, 13: 1419–1434.
- Lalli, C. M., and Gilmer, R. W. 1989. *Pelagic Snails: The Biology of Holoplanktonic Gastropod Mollusks*. Stanford University Press, Stanford, CA, USA. pp. 259.
- Lewis, G., and Nyman, J. S. 2008. The use of nanoindentation for characterizing the properties of mineralized hard tissues: state-of-the art review. *Journal of Biomedical Materials Research. Part B, Applied Biomaterials*, 87B: 286–301.
- Lischka, S., Büdenbender, J., Boxhammer, T., and Riebesell, U. 2011. Impact of ocean acidification and elevated temperatures on early juveniles of the polar shelled pteropod *Limacina helicina*: mortality, shell degradation, and shell growth. *Biogeosciences*, 8: 919–932.
- Lischka, S., and Riebesell, U. 2012. Synergistic effects of ocean acidification and warming on overwintering pteropods in the Arctic. *Global Change Biology*, 18: 3517–3528.
- Manno, C., Sandrini, S., Tositti, L., and Accornero, A. 2007. First stages of degradation of *Limacina helicina* shells observed above the aragonite chemical lysocline in Terra Nova Bay (Antarctica). *Journal of Marine Systems*, 68: 91–102.
- Manno, C., Morata, N., and Primicerio, R. 2012. *Limacina retroversa*'s response to combined effects of ocean acidification and sea water freshening. *Estuarine, Coastal and Shelf Science*, 113: 163–171.
- McNeil, B. I., and Matear, R. J. 2008. Southern Ocean acidification: A tipping point at 450-ppm atmospheric CO₂. *Proceedings of the National Academy of Sciences of the U S A*, 105: 18860–18864.
- Moy, A. D., Howard, W. R., Trull, T. W., and Bray, S. 2009. Reduced calcification in modern Southern Ocean planktonic foraminifera. *Nature Geoscience*, 2: 276–280.
- Mucci, J. 1983. The solubility of calcite and aragonite in seawater at various salinities, temperatures, and one atmosphere total pressure. *American Journal of Science*, 283: 780–799.
- Oliver, W. C., and Pharr, G. M. 1992. An improved technique for determining hardness and elastic modulus using load and displacement sensing indentation experiments. *Journal of Materials Research*, 7: 1564–1583.
- Orr, J. C., Fabry, V. J., Aumont, O., Bopp, L., Doney, S. C., Feely, R. A., Gnanadesikan, A., *et al.* 2005. Anthropogenic ocean acidification over the twenty-first century and its impact on calcifying organisms. *Nature*, 437: 681–686.
- Pommeranz, T., Hermann, C., and Kühn, A. 1982. Mouth angle of the rectangular midwater trawl (RMT1+8) during paying out and hauling. *Meeresforschung*, 29: 267–274.
- Riebesell, U., Zondervan, I., Rost, B., Tortell, P. D., Zeebe, R. E., and Morel, F. M. M. 2000. Reduced calcification of marine plankton in response to increased atmospheric CO₂. *Nature*, 407: 364–366.
- Ries, J. B., Cohen, A. L., and McCorkle, D. C. 2009. Marine calcifiers exhibit mixed responses to CO₂-induced ocean acidification. *Geology*, 37: 1131–1134.
- Rintoul, S. R., and Bullister, J. L. 1999. A late winter hydrographic section from Tasmania to Antarctica. *Deep-Sea Research I*, 46: 1417–1454.
- Roberts, D., Howard, W. R., Moy, A. D., Roberts, J. L., Trull, T. W., Bray, S. G., and Hopcroft, R. R. 2011. Interannual pteropod variability in sediment traps deployed above and below the aragonite saturation horizon in the Sub-Antarctic Southern Ocean. *Polar Biology*, 34: 1739–1750.
- Roe, H. S. J., Baker, A. de C., Carson, R. M., Wild, R., and Shale, D. M. 1980. Behaviour of the Institute of Oceanographic Science's rectangular midwater trawls: theoretical aspects and experimental observations. *Marine Biology*, 56: 247–259.
- Sabine, C. L., Feely, R. A., Gruber, N., Key, R. M., Lee, K., Bullister, J. L., Wanninkhof, R., *et al.* 2004. The oceanic sink for anthropogenic CO₂. *Science*, 305: 367–371.
- Sato-Okoshi, W., Okoshi, K., Sasaki, H., and Akiha, F. 2010. Shell structure of two polar pelagic molluscs, Arctic *Limacina helicina* and Antarctic *Limacina helicina antarctica* forma *antarctica*. *Polar Biology*, 33: 1577–1583.
- Spero, H. J., Bijma, J., Lea, D. W., and Bemis, B. E. 1997. Effect of seawater carbonate concentration on foraminiferal carbon and oxygen isotopes. *Nature*, 390: 497–500.
- Taylor, J. D., and Layman, M. 1972. The mechanical properties of bivalve (mollusca) shell structures. *Palaeontology*, 15: 73–87.
- Tsui, T. Y., Vlassak, J., and Nix, W. D. 1999. Indentation plastic displacement field: Part I. The case of soft films on hard substrates. *Journal of Materials Research*, 14: 2196–2203.
- Zhang, T., Yurong, M., Chen, K., Kunz, M., Tamura, N., Qiang, M., Xu, J., *et al.* 2011. Structure and mechanical properties of a pteropod shell consisting of interlocked helical aragonite nanofibres. *Angewandte Chemie*, 123: 10545–10549.
- Zondervan, I., Zeebe, R. E., Rost, B., and Riebesell, U. 2001. Decreasing marine biogenic calcification: a negative feedback on rising atmospheric pCO₂. *Global Biogeochemical Cycles*, 15: 507–516.